REFERENCES AND NOTES

1. K. E. Kamm and J. T. Stull, *Annu. Rev. Pharmacol. Toxicol.* **25**, 593 (1985); D. J. Hartshorne, in *Physiology of the Gastrointestinal Tract*, D. R. Johnson, Ed. (Raven, New York, ed. 2, 1987), vol. 1, pp. 423–482; J. R. Sellers and R. S. Adelstein, in *The Enzymes* P. Boyer and E. G. Krebs, Eds. (Academic Press, San Diego, CA, 1987), vol. 18, pp. 381–418.
2. K. A. Giuliano and D. L. Taylor, *Curr. Opin. Cell Biol.* **7**, 4 (1995); A. Huttenlocher, R. Sandborg, A. Horwitz, *ibid.*, p. 697.
3. B. Bradley and K. G. Morgan, *J. Physiol. (London)* **385**, 437 (1987).
4. T. Kitazawa, M. Masuo, A. P. Somlyo, *Proc. Natl. Acad. Sci. U.S.A.* **88**, 9307 (1991); S. Moreland, J. Nishimura, C. van Breeman, H. Y. Ahn, R. S. Moreland, *Am. J. Physiol.* **263**, C540 (1992).
5. K. Hirata *et al.*, *J. Biol. Chem.* **267**, 8719 (1992).
6. M. Noda *et al.*, *FEBS Lett.* **367**, 246 (1995).
7. C. Nobes and A. Hall, *Curr. Opin. Genet. Dev.* **4**, 77 (1994); Y. Takai, K. Sasaki, K. Tanaka, H. Nakanishi, *Trends Biochem. Sci.* **20**, 227 (1995).
8. M. Amano *et al.*, *Science* **271**, 648 (1996).
9. H. Mukai and Y. Ono, *Biochem. Biophys. Res. Commun.* **199**, 897 (1994).
10. T. Matsui *et al.*, *EMBO J.* **15**, 2208 (1996); T. Leung, E. Manser, L. Tan, L. Lim, *J. Biol. Chem.* **270**, 29051 (1995).
11. T. Satoh, M. Nakafuku, Y. Kaziro, *J. Biol. Chem.* **267**, 24149 (1992); F. McCormick, *Curr. Opin. Genet. Dev.* **4**, 71 (1994).
12. Abbreviations for the amino acid residues are: A, Ala; C, Cys; D, Asp; E, Glu; F, Phe; G, Gly; H, His; I, Ile; K, Lys; L, Leu; M, Met; N, Asn; P, Pro; Q, Gln; R, Arg; S, Ser; T, Thr; V, Val; W, Trp; and Y, Tyr.
13. Y. H. Chen *et al.*, *FEBS Lett.* **356**, 51 (1994).
14. H. Shimizu *et al.*, *J. Biol. Chem.* **269**, 30407 (1994).
15. S. Fields and O. Song, *Nature* **340**, 245 (1989); A. B. Vojtek, S. M. Hollenberg, J. A. Cooper, *Cell* **74**, 205 (1993).
16. H. F. Paterson *et al.*, *J. Cell Biol.* **111**, 1001 (1990); A. J. Ridley and A. Hall, *Cell* **70**, 389 (1992); *EMBO J.* **13**, 2600 (1994).
17. B. Yamamori *et al.*, unpublished data.
18. L. Trinkle-Mulcahy, K. Ichikawa, D. J. Hartshorne, M. J. Siegman, T. M. Butler, *J. Biol. Chem.* **270**, 18191 (1995).
19. M. Amano *et al.*, unpublished data.
20. K. Kimura *et al.*, unpublished data.
21. Extracts of bovine brain membranes were applied to 0.25-ml glutathione-Sepharose 4B columns containing GST-linked small GTPases loaded with guanine nucleotides (*8*). The columns were washed three times with 0.825 ml of buffer A [20 mM tris-HCl (pH 7.5), 1 mM EDTA, 1 mM dithiothreitol, 5 mM $MgCl_2$] containing 0.2 M NaCl, and bound proteins were eluted together with the GST fusion proteins by the addition of 0.825 ml of buffer A containing 10 mM glutathione.
22. Rabbit polyclonal antibodies to chicken MBS and to the 20-kD regulatory subunit were generated with the use of recombinant proteins (*14*). Antibodies to the 37-kD catalytic subunit were from Santa Cruz Biotechnology.
23. MLC phosphatase activity was assayed for 6 min at 30°C in 50 μl of reaction mixture [30 mM tris-HCl (pH 7.5), 30 mM KCl, 3 mM $MgCl_2$, 5 mM EDTA, 1 mM dithiothreitol, 5 μM ^{32}P-labeled MLC, and test samples] (*14*).
24. In vitro translation of plasmid pCRII encoding rat MBS (amino acids 1 to 976) was performed as described [T. Yamamoto, T. Matsui, M. Nakafuku, A. Iwamatsu, K. Kaibuchii, *J. Biol. Chem.* **270**, 30557 (1995)]. The [^{35}S]methionine-labeled products were mixed with glutathione–Sepharose 4B beads coated with GST-RhoA loaded with guanine nucleotides.
25. To express fusion proteins of small GTPases with the LexA DNA-binding domain, we constructed plasmids pLex–H-Ras, pLex-RhoA, and pLex-RhoA^{V14} (*15*). To express fusion proteins of rMBS-N and rMBS-C with the Gal4p acidic activation domain, we constructed pACTII–rMBS-N and pACTII–rMBS-C, respectively (*15*). The *Saccharomyces cerevisiae* reporter strain L40 [*MAT***a**, *trp1*, *leu2*, *his3*, *LYS2::(lexAop)$_4$-HIS3*, *URA::(lexAop)$_8$-lacZ*] was transformed with plasmids encoding the LexA fusion proteins and plasmids encoding the Gal4p fusion proteins (*15*). The transformants were plated on synthetic medium lacking histidine. If the LexA fusion protein interacts with the Gal4p fusion protein, the transformant can express the *HIS3* reporter gene and therefore grow in the absence of histidine.
26. To express Myc epitope–tagged MBS, we cloned the complementary DNA encoding rat MBS into pEF-BOS–Myc to yield pEF-BOS–Myc-MBS (*10*). COS-7 cells were transfected with pEF-BOS–Myc-MBS alone or together with pEF-BOS–HA-RhoA or pEF-BOS–HA-RhoA^{V14} (*10*). After 40 hours, the cells were collected and homogenized. The cytosolic and particulate fractions were prepared and subjected to quantitative immunoblot analysis with antibodies (9E10) to the Myc epitope (*10*).
27. cMBS-N and cMBS-C were expressed as maltose-binding protein fusion proteins in *Escherichia coli* and purified (*15*).
28. The kinase reaction was performed in 50 μl of kinase buffer [50 mM tris-HCl (pH 7.5), 2.8 mM EDTA, 6.5 mM $MgCl_2$, 0.16% CHAPS detergent] containing 10 μM [γ-^{32}P]ATP (60 to 80 GBq/mmol), purified Rho-kinase (10 ng of protein), and cMBS-N or cMBS-C (450 ng of protein). After incubation for 10 min at 30°C, the reaction mixture was boiled in SDS sample buffer and resolved by SDS-PAGE. The ^{32}P-labeled bands corresponding to MBS were visualized by autoradiography. Fold stimulation of MBS phosphorylation was determined with a Fuji image analyzer (BAS-2000).
29. Myosin phosphatase was purified from chicken gizzard (*14*).
30. Thiophosphorylation of myosin phosphatase (1 μg) was performed in 50 μl of kinase buffer in the presence of 10 μM [^{35}S]ATP-γ-S (8 to 10 GBq/mmol) (*28*). After incubation for 6 min at 30°C, a portion of the mixture (40 μl) was subjected to SDS-PAGE and the remaining portion was assayed for MLC phosphatase activity (*23*).
31. NIH 3T3 cells were stably transfected with p3′SS (repressor plasmid) (Stratagene) and pOPRSVI–HA-RhoA or pOPRSVI–HA-RhoA^{V14} to establish cell lines overexpressing RhoA (RhoA-5 and RhoA-24 cell lines) or RhoA^{V14} (RhoA^{V14}-7 and RhoA^{V14}-25 cell lines) under the control of IPTG [D. L. Wyborski and J. M. Short, *Nucleic Acids Res.* **19**, 4647 (1991)].
32. Confluent NIH 3T3 cells (parental and RhoA-5, RhoA-24, RhoA^{V14}-7, and RhoA^{V14}-25 cell lines) in 35-mm dishes were treated with 5 mM IPTG for 24 hours. During the last 12 hours, the cells were deprived of serum, and during the last 2 hours they were labeled with 9.25 MBq of [^{32}P]orthophosphate. The cells were then lysed and MBS was immunoprecipitated. The washed immunoprecipitates were subjected to SDS-PAGE and autoradiography. Fold stimulation of MBS phosphorylation was determined with a Fuji BAS-2000 image analyzer. Under similar conditions, with the exception that the cells were not labeled, cells were lysed and the lysates were subjected to immunoblot analysis with antibodies to MBS and RhoA.
33. IPTG-treated, serum-deprived NIH 3T3 cell lines (100-mm dishes) were treated with 10% (w/v) trichloroacetic acid. The resulting precipitates were subjected to glycerol-urea gel electrophoresis, and the relative amounts of nonphosphorylated and phosphorylated forms of MLC were determined by immunoblot analysis [D. A. Taylor and J. T. Stull, *J. Biol. Chem.* **263**, 14456 (1988)]. NIH 3T3 cells were treated with 0.1 μM calyculin A for 10 min.

34. We thank M. Fujioka and J. Tanaka for preparing polyclonal antibodies to MBS and the 20-kD regulatory subunit of myosin phosphatase, Y. Hamajima for preparing NIH 3T3 cell lines, M. Inagaki for valuable discussions, and M. Nishimura for help in preparing the manuscript. Supported by grants-in-aid for scientific research and for cancer research from the Ministry of Education, Science, and Culture of Japan.

28 March 1996; accepted 20 May 1996

Bipartite Ca^{2+}-Binding Motif in C_2 Domains of Synaptotagmin and Protein Kinase C

Xuguang Shao, Bazbek A. Davletov,* R. Bryan Sutton, Thomas C. Südhof, Josep Rizo†

C_2 domains are found in many proteins involved in membrane traffic or signal transduction. Although C_2 domains are thought to bind calcium ions, the structural basis for calcium binding is unclear. Analysis of calcium binding to C_2 domains of synaptotagmin I and protein kinase C–β by nuclear magnetic resonance spectroscopy revealed a bipartite calcium-binding motif that involves the coordination of two calcium ions by five aspartate residues located on two separate loops. Sequence comparisons indicated that this may be a widely used calcium-binding motif, designated here as the C_2 motif.

Calcium ions regulate a wide variety of biological functions through binding to proteins. Most Ca^{2+}-binding proteins can be grouped into families with common structural motifs such as the EF-hand motif (*1*). A structural unit called the C_2 domain, first defined in protein kinase C (PKC) (*2*), has recently been recognized as a widespread domain that may participate in numerous Ca^{2+}-regulatory roles. More than 50 C_2 domains have been identified in various proteins, many of which participate in signal transduction or membrane traffic (*3*). Although Ca^{2+}-dependent binding of some of these proteins to phospholipids or to other proteins has been shown (*4*–*7*), the generality and structural basis of Ca^{2+} binding to C_2

X. Shao and J. Rizo, Department of Pharmacology, and R. B. Sutton, Department of Biochemistry, University of Texas Southwestern Medical Center, 5323 Harry Hines Boulevard, Dallas, TX 75235, USA.

sw;6.75qB. A. Davletov and T. C. Südhof, Department of Molecular Genetics and Howard Hughes Medical Institute, University of Texas Southwestern Medical Center, 5323 Harry Hines Boulevard, Dallas, TX 75235, USA.

*Present address: Department of Biochemistry, Imperial College of Science, Technology and Medicine, London SW7 2AY, UK.

†To whom correspondence should be addressed.

domains remains unclear.

Synaptotagmin I is a synaptic vesicle protein that contains two C_2 domains and plays a key role in Ca^{2+}-evoked neurotransmitter release (*8*). The first C_2 domain of synaptotagmin I (hereafter referred to as the C_2A domain) binds phospholipids (*7*) and syntaxin (*6*) in a Ca^{2+}-dependent manner. The crystal structure of the C_2A domain has been solved (*9*), revealing a compact β-sandwich fold formed by two four-stranded antiparallel β sheets (see below). Diffusion of Ca^{2+} into the crystals allowed identification of a single Ca^{2+} ion bound to a site formed by two loops and coordinated by residues Asp^{172}, Asp^{178}, Asp^{230}, and Asp^{232}. However, only Asp^{178} and Asp^{230} were well ordered, and the crystals cracked when more than 100 μM Ca^{2+} was present (*9*). It thus remained unclear how the C_2A domain binds Ca^{2+} and whether conformational changes are hindered by crystal contacts. In addition, the cooperativity observed in phospholipid binding suggests that the C_2A domain binds at least two Ca^{2+} ions (*7*). To elucidate how the C_2A domain of synaptotagmin I binds Ca^{2+} and how general its Ca^{2+}-binding mode is, we used nuclear magnetic resonance (NMR) spectroscopy in solution.

We obtained complete assignments of the ^1H and ^{15}N resonances of the backbone and of 70% of the side chains of the C_2A domain at pH 5.0 in the absence and presence of Ca^{2+} (*10*, *11*). The ^1H-^{15}N heteronuclear single-quantum correlation (HSQC) spectra of the Ca^{2+}-free and Ca^{2+}-bound forms of the C_2A domain at pH 5.0 are shown in Fig. 1. All larger Ca^{2+}-induced chemical shift changes in these spectra

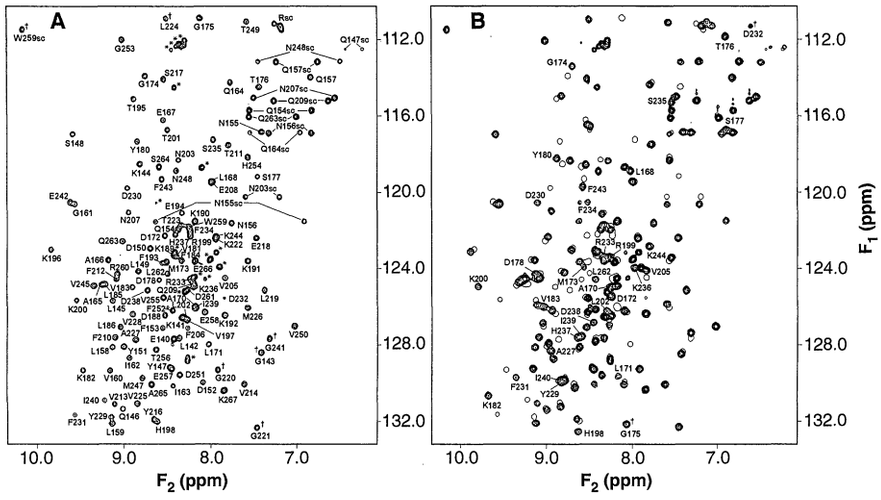

Fig. 1. ^1H-^{15}N HSQC spectra of the C_2A domain at 34°C and pH 5.0 in the absence (**A**) and presence (**B**) of Ca^{2+} (*24*). For comparison, the HSQC spectrum in (A) is superimposed in (B), drawing single contours. Cross peak assignments are indicated in (A) (sc, side chain). Only cross peaks with significant shifts are labeled in (B). A dagger indicates cross peaks that are folded along the F_1 dimension and an asterisk indicates cross peaks from a 17-residue NH_2-terminal sequence from the expression vector used; ppm, parts per million.

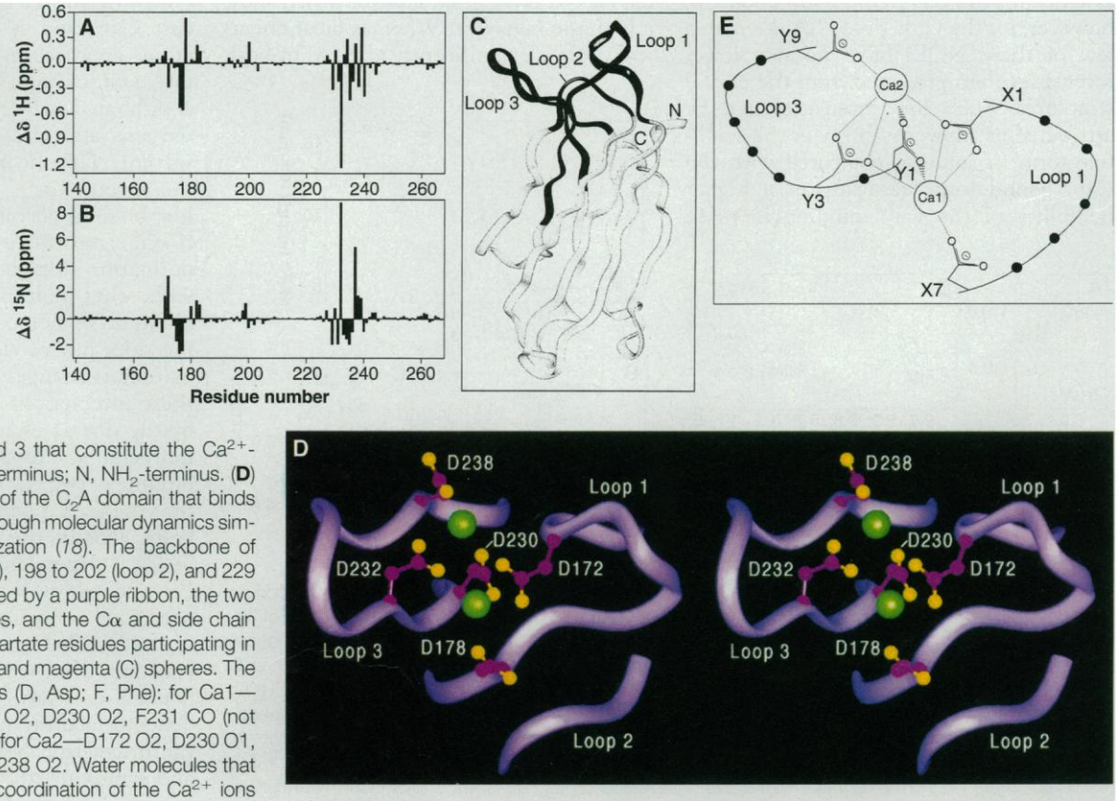

Fig. 2. Model of the bipartite Ca^{2+}-binding motif of the C_2A domain. Changes in backbone amide ^1H (**A**) and ^{15}N (**B**) chemical shifts induced by Ca^{2+} binding to the C_2A domain ($\Delta\delta = \delta_{+Ca} - \delta_{-Ca}$). (**C**) Ribbon diagram of the crystal structure of the C_2A domain (*9*) showing the regions with the largest Ca^{2+}-induced chemical shift changes (shaded black). These regions (residues 168 to 183, 198 to 202, and 227 to 240) include the loops labeled 1, 2, and 3 that constitute the Ca^{2+}-binding region. C, COOH-terminus; N, NH_2-terminus. (**D**) Stereo picture of the motif of the C_2A domain that binds two Ca^{2+} ions, obtained through molecular dynamics simulation and energy minimization (*18*). The backbone of residues 170 to 180 (loop 1), 198 to 202 (loop 2), and 229 to 240 (loop 3) is represented by a purple ribbon, the two Ca^{2+} ions by green spheres, and the Cα and side chain heavy atoms of the five aspartate residues participating in Ca^{2+} binding by yellow (O) and magenta (C) spheres. The Ca^{2+} ligands are as follows (D, Asp; F, Phe): for Ca1—D172 O1, D172 O2, D178 O2, D230 O2, F231 CO (not shown), and D232 O1; and for Ca2—D172 O2, D230 O1, D232 O1, D232 O2, and D238 O2. Water molecules that presumably complete the coordination of the Ca^{2+} ions were not included in the calculations. (**E**) General model of Ca^{2+} binding by C_2 motifs. The Ca^{2+}-binding residues in loop 1 are labeled X1 and X7 and those in loop 3 are labeled Y1, Y3, and Y9; these residues are most often aspartates but may also be glutamates and sometimes asparagine [see sequence alignment in (*3*)]. Solid circles represent residues between the aspartate residues.

(Fig. 2, A and B) are observed in the loops labeled 1 to 3 in the ribbon diagram (Fig. 2C), showing that Ca^{2+} binding is restricted to this region of the C_2A domain. Many of the largest changes are observed for amide protons near the four aspartate residues that bind the Ca^{2+} ion in the crystal structure. However, large chemical shift changes are also observed around Asp^{238}, which is more distant from this bound Ca^{2+} ion and does not participate in its binding. These observations led us to hypothesize that the C_2A domain binds a second Ca^{2+} ion at a cavity formed by the side chains of Asp^{172}, Asp^{230}, Asp^{232}, and Asp^{238} as shown in our model (Fig. 2D).

Our model (Fig. 2D) is based on the assumptions that the solution structure of the C_2A domain is very similar to its crystal structure and that Ca^{2+} binding does not produce substantial conformational changes. We tested these assumptions by analyzing more than 1300 nuclear Overhauser effects (NOEs) assigned for Ca^{2+}-free and Ca^{2+}-bound C_2A domains (*12*). The NOE patterns observed for both forms are very similar and agree well with the interproton distances predicted from the crystal structures (*13*). The excellent correlation with the crystal structures includes 46 long-range NOEs involving protons in loops 1 through 3 that have been assigned for the Ca^{2+}-bound C_2A domain; however, for the Ca^{2+}-free C_2A domain, a few of these NOEs have notably lower intensities than predicted from the crystal structures. Such low intensities can be attributed to a lower stability of the Ca^{2+}-free form in solution compared with the Ca^{2+}-bound form, resulting in a higher flexibility of the Ca^{2+}-binding loops in the absence of Ca^{2+}. Structural stabilization due to Ca^{2+} binding was confirmed by the observation of a Ca^{2+}-induced shift in the denaturation temperature from 55°C to 74°C. Stabilization is consistent with a slight Ca^{2+}-induced change observed in the circular dichroism (CD) spectrum of the C_2A domain (*14*), as well as with increased resistance to proteolysis (*15*). These results indicate that the solution structure and the crystal structure of the C_2A domain are very similar and show that Ca^{2+} binding stabilizes the structure of the C_2A domain without inducing a substantial conformational change.

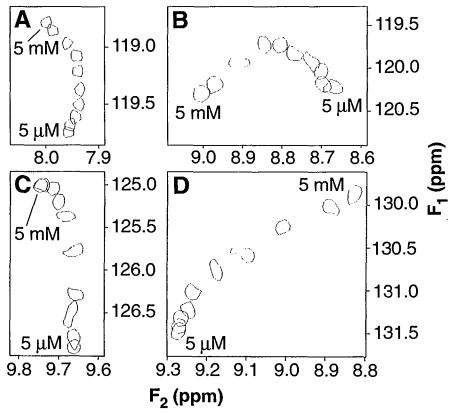

Fig. 3. The C_2A domain binds two Ca^{2+} ions. A Ca^{2+} titration of uniformly ^{15}N-labeled C_2A domain (100 μM) was monitored through use of ^1H-^{15}N HSQC spectra (*16*). Expansions of the 10 HSQC spectra showing the evolution of the amide cross peaks from Leu^{168} (**A**), Asp^{230} (**B**), Lys^{200} (**C**), and Ile^{240} (**D**) are superimposed to illustrate the biphasic shift behavior.

To test the Ca^{2+}-binding model proposed (Fig. 2D), we performed a Ca^{2+} titration experiment monitored by HSQC spectra at pH 7.4 (*16*). Many HSQC cross peaks moved nonlinearly during the titration from their positions in the Ca^{2+}-free state to their positions in the fully Ca^{2+}-saturated state (Fig. 3), demonstrating that at least one intermediate, partially saturated state exists. A straightforward explanation is that the intermediate state or states arise from the binding of a single Ca^{2+} ion, whereas full saturation involves the binding of two Ca^{2+} ions. This conclusion is supported by plots of the dependence of the ^1H or ^{15}N chemical shift on the Ca^{2+} concentration for each individual HSQC cross peak, most of which show a biphasic behavior. Whereas most chemical shifts are significantly affected by both Ca^{2+} ions, the ^{15}N chemical shift of the Lys^{200} NH group is primarily influenced by Ca^{2+} binding to the higher affinity site, and the ^1H chemical shift of the Ile^{240} NH group is mostly affected by binding to the lower affinity site (Fig. 3, C and D), thus allowing accurate measurements of the two dissociation constants. Curve fitting yielded dissociation constant (K_D) values of 60 and 400 μM, in agreement with the values estimated from the other titration curves and from titrations monitored through use of CD and thermal denaturation (*14, 17*). The two-Ca^{2+} ion-binding model was also supported by measurements of Mn^{2+}-induced intensity changes in the HSQC cross peaks of the C_2A domain (caused by paramagnetic relaxation effects upon Mn^{2+} binding), which were well correlated with the distances from the NH groups to the closest Mn^{2+} ion predicted by the model (*12*). Finally, molecular dynamics simulations showed that Ca^{2+} ions placed in front of loops 1 through 3 move spontaneously into the two predicted binding sites (Fig. 2D) (*18*).

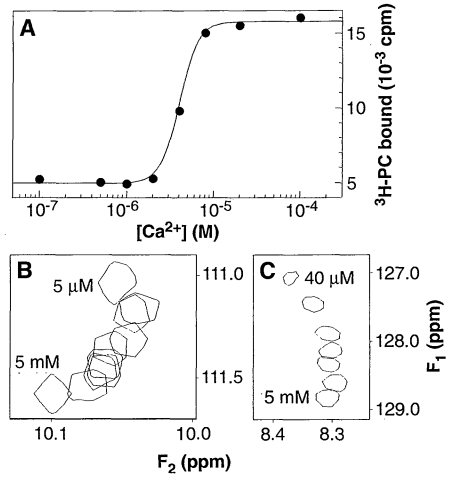

Fig. 4. Ca^{2+}-binding properties of the C_2 domain of PKC-β. (**A**) Ca^{2+}-dependent binding of the PKC-β C_2 domain to ^{3}H-labeled phosphatidylcholine (PC)-containing liposomes (*22*). (**B** and **C**) Ca^{2+} titration of uniformly ^{15}N-labeled PKC-β C_2 domain (40 μM) monitored with HSQC spectra (*23*). Expansions of a superposition of the 10 HSQC spectra illustrating the evolution of two amide cross peaks are shown (Ca^{2+} concentrations were the same as for titration of the C_2A domain). The cross peak in (C) was not observed at Ca^{2+} concentrations below 40 μM.

Altogether, our results show that the C_2A domain binds two Ca^{2+} ions as described in the model (Fig. 2D). In this model Asp^{172}, Asp^{230}, and Asp^{232} act as bidentate ligands that coordinate with the two Ca^{2+} ions, forming a triangle with a Ca^{2+} ion on each side; Asp^{178} and Asp^{238} bind only one Ca^{2+} ion each. Whereas the first Ca^{2+} ion is surrounded by oxygen atoms approaching a hexa- or heptadentate coordination, the second Ca^{2+} ion is coordinated with only five carboxylate oxygens and is partially exposed to the solvent. The incomplete coordination of the second Ca^{2+} ion correlates with its low binding affinity and may have functional significance because the empty coordination sites may mediate interactions with other molecules, for example, phospholipids or syntaxin. Because Ca^{2+} binding does not produce substantial conformational changes in the C_2A domain, these interactions are likely to be driven by the drastic change in electrostatic potential around loops 1 through 3 caused by binding of two Ca^{2+} ions. The observation that the C_2A domain binds two Ca^{2+} ions helps explain the cooperativity observed in Ca^{2+}-dependent phospholipid binding (*7*) and fits well with the cooperativity observed in synaptic vesicle exocytosis (*19, 20*). The intrinsic Ca^{2+} dissociation constants that we measured for the C_2A domain correlate with the Ca^{2+} dependence of neurotransmitter release (*19*), of the interaction between the C_2A domain and syntaxin (*6*), and of the self-association of the second C_2 domain of synaptotagmin I (*20*). These observations provide further support for a function of synapto-

tagmin I as a Ca^{2+} sensor in neurotransmitter release (*8*).

The bipartite Ca^{2+}-binding motif of the C_2A domain, which we designate the C_2 motif, involves five aspartate residues observed in an identical pattern in many but not all C_2 domains (*3*). Hence, these C_2 domains may share the two-Ca^{2+} ion-binding motif present in the C_2A domain of synaptotagmin I. To test this postulate, we analyzed the C_2 domain of PKC-β with the key experiments that defined the Ca^{2+}-binding properties of the C_2A domain of synaptotagmin I. Although the C_2 domain of PKC is believed to be involved in its Ca^{2+}-dependent phospholipid binding properties (*2*), it has been suggested that this domain is not sufficient for Ca^{2+} binding (*21*). However, when we tested for this directly we found that the PKC-β C_2 domain alone is capable of binding phospholipids in a Ca^{2+}-dependent manner, with affinity and cooperativity similar to those observed for the C_2A domain of synaptotagmin I (*7*, *22*) (Fig. 4A). Analysis by CD also showed a small Ca^{2+}-induced spectral change for the PKC-β C_2 domain and a shift in denaturation temperature from 48°C to 74°C. A Ca^{2+} titration of the PKC-β C_2 domain at pH 7.4 monitored by HSQC spectra revealed nonlinear movement of some cross peaks from the Ca^{2+}-free positions to the fully Ca^{2+}-bound positions (Fig. 4, B and C) (*23*), showing that the PKC-β C_2 domain binds at least two Ca^{2+} ions. These results clearly establish that the PKC-β C_2 domain is an autonomous Ca^{2+}-binding domain and support the proposal that its Ca^{2+}-binding mode is analogous to that of the C_2A domain of synaptotagmin I.

The analogous Ca^{2+}-binding properties of the two C_2 domains studied here, together with the conservation of the five aspartate residues in many C_2 domain proteins, strongly indicate that the C_2 motif constitutes a widely used Ca^{2+}-binding motif. This motif is different from the EF-hand motif, which binds a single Ca^{2+} ion and is formed by a contiguous polypeptide chain in a helix-loop-helix arrangement (*1*). The C_2 motif binds two Ca^{2+} ions through two loops that are distant in the sequence, with a third small loop playing a supporting role. The motif is built at the tip of a stable β-sandwich structure that allows clustering of five negative charges in a relatively small region. The fundamental signature of the C_2 motif includes two residues from loop 1 (separated by 5 ± 1 residues) and three residues from loop 3 (separated by 1 and by 5 ± 1 residues) (Fig. 2E). Note the pseudosymmetry of the motif (Fig. 2E), where a C_2 axis relates Ca1 to Ca2, X1 to Y3 and X7 to Y9. The structure of the C_2 motif revealed here provides an explanation for the Ca^{2+}-binding properties observed in proteins bearing C_2 domains (*4*–*7*) and suggests a mechanistic basis for the action of many regulatory proteins involved in membrane traffic and signal transduction.

REFERENCES AND NOTES

1. N. C. J. Strynadka and M. N. G. James, *Annu. Rev. Biochem.* **58**, 951 (1989).
2. Reviewed in Y. Nishizuka, *Science* **258**, 607 (1992); A. Newton, *Annu. Rev. Biophys. Biomol. Struct.* **22**, 1 (1993).
3. N. Brose, K. Hofmann, Y. Hata, T. C. Südhof, *J. Biol. Chem.* **270**, 25273 (1995).
4. N. Brose, A. G. Petrenko, T. C. Südhof, R. Jahn, *Science* **256**, 1021 (1992); B. Ullrich *et al.*, *Neuron* **13**, 1281 (1994).
5. J. D. Clark *et al.*, *Cell* **65**, 1043 (1991); T. Yamaguchi *et al.*, *J. Biol. Chem.* **268**, 27164 (1993).
6. C. Li *et al.*, *Nature* **375**, 594 (1995).
7. B. A. Davletov and T. C. Südhof, *J. Biol. Chem.* **268**, 26386 (1993).
8. M. S. Perin, V. A. Fried, G. A. Mignery, R. Jahn, T. C. Südhof, *Nature* **345**, 260 (1990); M. Geppert *et al.*, *Cell* **79**, 717 (1994); reviewed in T. C. Südhof, *Nature* **375**, 645 (1995).
9. R. B. Sutton, B. A. Davletov, A. M. Berghuis, T. C. Südhof, S. R. Sprang, *Cell* **80**, 929 (1995).
10. The plasmid encoding the C_2A domain of rat synaptotagmin I (residues 140 through 267) as a glutathione-S-transferase (GST) fusion was described previously (*7*). The isolated C_2A domain was obtained by expression in *Escherichia coli* BL21(DE3) cells, purification through affinity chromatography on glutathione-agarose beads, cleavage with thrombin, and purification through gel filtration on Superdex-75 (Pharmacia). Uniform ^{15}N labeling was achieved by growing the bacteria in M9 minimal medium containing $^{15}NH_4Cl$ as the sole nitrogen source. All NMR spectra were recorded on a Varian Unity-500 spectrometer. Data on 1 mM C_2A domain samples were obtained at 34°C and pH 5.0 (40 mM perdeuterated acetate, 100 mM NaCl) in 0.2 mM EGTA or 30 mM $CaCl_2$. Assignments under each condition were obtained through two-dimensional (2D) double-quantum filtered correlation spectroscopy, 2D total correlation spectroscopy (TOCSY), 2D NOE spectroscopy (NOESY), 2D ^1H-^{15}N HSQC, 3D ^1H-^{15}N TOCSY–heteronuclear multiple quantum correlation (TOCSY-HMQC), and 3D ^1H-^{15}N NOESY-HMQC experiments [for original references see A. M. Gronenborn and G. M. Clore, *Anal. Chem.* **62**, 2 (1990), and for experimental details see J. Rizo, Z.-P. Liu, L. M. Gierasch, *J. Biomol. NMR* **4**, 741 (1994)].
11. We also obtained assignments for all observable ^1H and ^{15}N backbone resonances at 25°C near physiological pH (40 mM perdeuterated tris, pH 7.4, and 100 mM NaCl) in 0.2 mM EGTA or 15 mM $CaCl_2$. The similarity of the chemical shifts and NOE patterns observed at pH 5.0 and 7.4 indicates that no significant differences exist between the structures of the C_2A domain at these two pHs.
12. X. Shao, B. A. Davletov, R. B. Sutton, T. C. Südhoff, J. Rizo, unpublished results.
13. The crystal structures of the C_2A domain obtained in the absence of Ca^{2+} and after diffusing 100 μM Ca^{2+} into the crystals (*9*) are nearly identical (Cα root mean square deviation 0.2 Å), and the interproton distances predicted from them are similar (within 0.2 Å); differences larger than 0.5 Å are observed in very few cases.
14. The CD spectrum of 8 μM C_2A domain in 0.2 mM EGTA and 10 mM tris (pH 7.7) was typical of a β sheet protein, with a minimum at 218 nm and a maximum at 203 nm. Addition of 5 mM Ca^{2+} caused a slight decrease in the intensity of the minimum and a slight increase in the maximum. Thermal denaturation in 0.2 mM EGTA or 5 mM Ca^{2+} was monitored through the CD absorption at 204 nm. Ca^{2+} titrations monitored by CD or by thermal denaturation indicated half-maximal binding with 200 to 300 μM Ca^{2+}. These experiments were performed on an Aviv Model 62DS spectropolarimeter.
15. B. A. Davletov and T. C. Südhof, *J. Biol. Chem.* **269**, 28547 (1994).
16. ^1H-^{15}N HSQC spectra were acquired on a 100 μM ^{15}N-labeled C_2A domain sample at pH 7.4 and 25°C in a 9:1 ratio of H_2O and D_2O containing 10 mM perdeuterated tris and 75 mM NaCl and with total Ca^{2+} concentrations of 5, 20, 40, 80, 140, 250, 400, and 800 μM and 2 and 5 mM (21 hours per spectrum).
17. These affinities also explain the fact that only one bound Ca^{2+} ion was observed in the crystal structure in the presence of 100 μM Ca^{2+} (*9*).
18. Simulations (30 ps) were performed on a Silicon Graphics Indigo^2 workstation with the program Discover (Biosym Technologies). A 1-fs time step, a 15.0 Å cutoff for nonbonding interactions, and a distance-dependent dielectric constant were used. Structures taken at 1 ps along the trajectories were energy minimized. A first simulation was performed starting with the Ca^{2+}-bound crystal structure in which the Ca^{2+} ion was pulled 18 Å away and only the Ca^{2+} ion and the five aspartate side chains were allowed to move: The Ca^{2+} ion moved into the binding site observed in the crystals. In a simulation in which a second Ca^{2+} ion was added, also 18 Å away, the ion moved into the second binding site predicted. In a final simulation with a third Ca^{2+} ion, the ion was repelled to infinity.
19. Exocytosis requires binding of at least three to four Ca^{2+} ions for activation and is half-maximal at 200 μM Ca^{2+} [R. Heidelberger, C. Heinemann, E. Neher, G. Mathews, *Nature* **371**, 513 (1994)].
20. Note that synaptotagmin I contains a second C_2 domain that also appears to be Ca^{2+} regulated [S. Sugita, Y. Hata, T. C. Südhof, *J. Biol. Chem.* **271**, 1262 (1996)].
21. J.-H. Luo and I. B. Weinstein, *J. Biol. Chem.* **268**, 23580 (1993).
22. A pGex-KG expression vector encoding a GST fusion with the C_2 domain of PKC-β (residues 157 to 289) was constructed by polymerase chain reaction as described for the C_2A domain (*7*) with the oligonucleotides GCCCCATGGAGCGCCGTGGCCGCATCT and GGCAAGCTTACGGCACATTAAAGTACTCG. Ca^{2+}-dependent phospholipid binding was analyzed with the GST–PKC-β C_2 domain fusion protein attached to glutathione-agarose beads with ^3H-labeled liposomes essentially as described (*7*). Half-maximal binding was observed with 4.2 μM Ca^{2+} with a Hill coefficient of 3.0 to 4.0.
23. A series of sensitivity-enhanced ^1H-^{15}N HSQC spectra [O. Zhang, L. E. Kay, J. P. Olivier, J. D. Forman-Kay, *J. Biomol. NMR* **4**, 845 (1994)] were acquired on a 40-μM, uniformly ^{15}N-labeled PKC-β C_2 domain sample under conditions analogous to those described (*16*) (10 hours per experiment). The PKC-β C_2 domain has a somewhat higher Ca^{2+} affinity than the C_2A domain of synaptotagmin I, resulting in a slower exchange between the Ca^{2+}-free and Ca^{2+}-bound states. Thus, only a few crosspeaks with small Ca^{2+}-induced shifts could be monitored throughout the titration.
24. Abbreviations for the amino acid residues are as follows: A, Ala; C, Cys; D, Asp; E, Glu; F, Phe; G, Gly; H, His; I, Ile; K, Lys; L, Leu; M, Met; N, Asn; P, Pro; Q, Gln; R, Arg; S, Ser; T, Thr; V, Val; W, Trp; and Y, Tyr.

25. We thank S. Sprang and C. Li for fruitful discussions and L. Kay for providing the sensitivity-enhanced HSQC pulse sequence. Supported by a joint grant from the William Randolph Hearst Foundation and the United Cerebral Palsy Research and Educational Foundation (J.R.), by a grant from the Welch Foundation (J.R.), and by NIH grants R29 NS33731-01A1 (J.R.) and RO1-MH52804-01 (T.C.S.).

3 March 1996; accepted 30 April 1996